STU SvF
SLOVAK UNIVERSITY OF TECHNOLOGY IN BRATISLAVA
FACULTY OF CIVIL ENGINEERING

Slovak Journal of Civil Engineering

Vol. 34, 2026, No. 1, 13 –20
DOI: 10.2478/sjce-2026-0002

NONLINEAR ANALYSIS OF A PRESTRESSED BEAM SUBJECTED TO SHEAR STRESS

Jaroslav BARAN [1*], Viktor BORZOVIČ [1], Fernando GONZALEZ-VIDOSA [2]

Article history

Received 23 September 2025
Revised 12 December 2025
Accepted 20 January 2026

Abstract

Nonlinear finite element modelling is a standard tool for the extension of experimental research programs in the field of the design of concrete load-bearing structures. It allows for the expansion of the database of results obtained by a demanding experimental test in order to monitor quantities that could not be recorded during experiments and thus to formulate further conclusions from the research. The paper deals with an analysis of the shear stress of prestressed concrete beams with shear reinforcement. It is focused on investigating the effect of the magnitude of the axial force on the shear resistance. A beam with a height of 0.6 m and an I-shaped cross-section was analysed. A prestressed beam is used as a typical load-bearing element for the construction of road bridges. Two types of models were used: one considered the reinforcement as a discrete element and the second as a model with a smeared reinforcement. The modelling results confirmed only a small effect of the axial force on the increase in shear resistance.

Address

1 Faculty of Civil Engineering, Slovak University of Technology in Bratislava, Bratislava .
2 ICITECH, Universitat Politècnica de València, Valencia, Spain

* ***Corresponding author:*** jaroslav.baran@stuba.sk

Key words

- Shear Resistance,
- Shear Reinforcement,
- Prestressed Beam,
- Nonlinear Analysis.

1 INTRODUCTION

This paper presents a parametric study investigating the shear resistance of prestressed concrete beams with bonded strands. The primary focus is on the effect of the prestressing level on the shear resistance of specimens with two different shear reinforcement ratios (Rupf 2013, Huber 2018, Hillebrand 2019). The variations in the prestressing level are intended to represent the loss of prestressing in existing concrete elements due to creep, shrinkage and material degradation, the corrosion of prestressing units (Belletti 2020, Moravčík 2020), or the simulation of the difference between a prestressed and reinforced concrete element (Herbrand 2013, Herbrand 2017). The amount of longitudinal reinforcement and the material characteristics of the concrete and reinforcing steel were kept constant across all the specimens investigated.

This parametric study processes the results from two distinct Finite Element Method (FEM) computational models. One is an FEM model with discretely modelled reinforcement and prestressing units, which was analysed using Atena software (Červenka 2017). The second is an FEM model with smeared reinforcement and prestressing units, which was analysed using the UPV model developed by Fernando Gonzalez-Vidosa (Vidosa 1989). Both models were calibrated based on the results of the experimental testing of prestressed beams.

2 EXPERIMENTAL SPECIMEN – A PRESTRESSED CONCRETE BEAM

The prestressed I-beam analysed has a height of 0.6 m and an overall length of 7.0 m. The beam´s cross-section is a standardized one commonly used in road bridge construction, and is designated as ´´VP-DPS´´. The basic geometric properties of the specimen are presented in Table 1, and its structural scheme is shown in Figure 1.

Tab. 1 *Geometric characteristics of the specimen*

Beam VP-DPS 600			
Total length	L_{beam}	7.000	[m]
Cross-section height	H_{beam}	0.600	[m]
Max. width of cross-section	$b_{max,beam}$	0.600	[m]
Min. width of cross-section	$b_{min,beam}$	0.180	[m]
Cross-section area	$A_{c,beam}$	0.209	[m^2]
Total weight of beam	G_{beam}	3.675	[t]

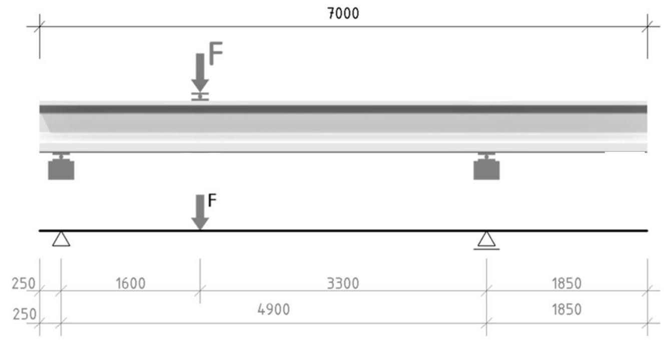

Fig. 1 *Structural scheme of the specimen – 3-point loading scheme*

2.1 Geometry of the specimen

The beam´s cross-section is I-shaped with a bottom flange width of 540 mm and a top flange width of 600 mm. The web width of the beam is 180 mm. The geometry of the cross-section is illustrated in Figure 2.

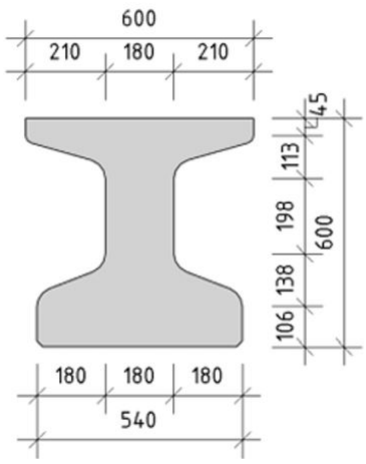

Fig. 2 *Cross-section of the specimen*

The cross-section properties of the beams tested are presented in Table 2. Figure 3 shows the shear-stressed area between the loading force and the edge support. Widths of 150 mm of the supporting and loading elements are indicated.

Tab. 2 *Cross-sectional characteristics of the concrete section*

Beam VP-DPS 600			
Moment of inertia	$I_{y,c}$	8.613×10^{-3}	[m^4]
Elastic section modulus – top	$W_{y,top}$	2.717×10^{-2}	[m^3]
Elastic section modulus – bottom	$W_{y,bottom}$	3.043×10^{-2}	[m^3]
Effective depth for prestressing steel	d_p	515	[mm]
Effective depth for reinforcing steel	d_s	563	[mm]
Effective depth of cross-section	d	547	[mm]
Web width	b_w	180	[mm]
Distance of force from support face	a	1450	[mm]
Shear slenderness	a/d	2.65	[-]
Longitudinal reinforcement ratio	ρ_l	3.13	[%]
Shear reinforcement ratio – Beam N1	$\rho_{w,N1}$	0.477	[%]
Shear reinforcement ratio – Beam N2	$\rho_{w,N2}$	0.105	[%]

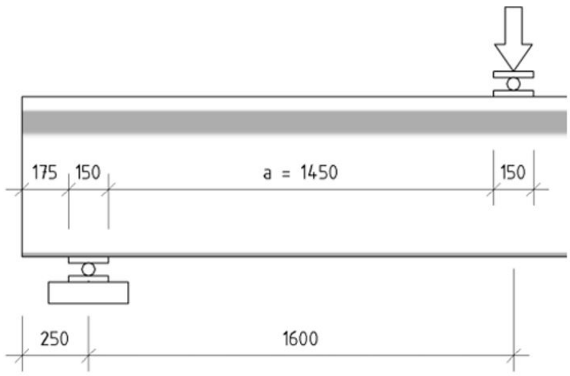

Fig. 3 *Geometry of beam support and load position applied*

2.2 Material properties

The properties of the material are listed based on the results of testing samples of the materials used.

Concrete

Table 3 shows the strength and deformation properties of the concrete as the average result of at least three samples. The value of the tensile strength was derived from the cylindrical strength according to Eurocode 2.

Tab. 3 *Material characteristics of the concrete*

Concrete			
Cube´s compressive strength	$f_{c,cube}$	61.53	[MPa]
Cylindrical compressive strength	$f_{c,cyl} = f_c$	43.58	[MPa]
Tensile strength	f_{ct}	3.72	[MPa]
Modulus of elasticity	E_c	35.18	[GPa]

The Reinforcing and prestressing steel

The beam is reinforced with longitudinal bars of diameters of 20 mm and 10 mm. It incorporates 10 bonded 7-wire prestressing strands, each with a diameter of 15.7 mm. In all the specimens, the longitudinal reinforcement ratio (ρ_l) maintains a value of 3.13 %, according to the following equation (1):

$$\rho_l = \frac{A_{p,bottom} + A_{s,bottom}}{b_w \cdot d} = 3.13\ \% \tag{1}$$

The specimens are categorized into two types, i.e., N1 and N2, based on their shear reinforcement ratios ρsw. Specimen N1, with a shear reinforcement ratio $\rho_{sw,N1}$ of 0.477%, is reinforced with double-leg stirrups of an 8 mm diameter spaced at 125 mm. Specimen N2, with a shear reinforcement ratio $\rho_{sw,N2}$ of 0.105%, is reinforced with double-leg stirrups of a 6 mm diameter spaced at 300 mm. The beam reinforcement was designed to allow for two experimental tests on a single beam. The reinforcement arrangement of the beam is shown in Figure 4.

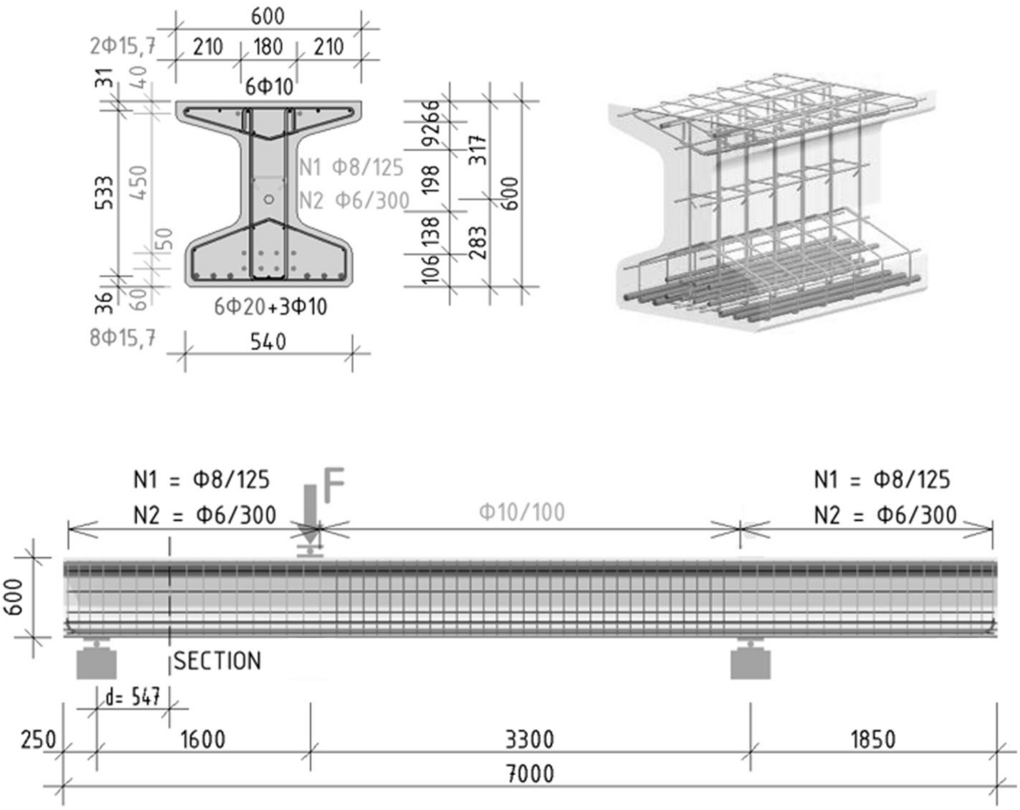

Fig. 4 Reinforcement arrangement of the specimens: cross-section (top left), 3D view (top right), Side view (bottom)

Table 4 shows the material properties of the reinforcing steel. Table 5 presents the material properties of the prestressing strands.

Tab. 4 *Material characteristics of the concrete*

Reinforcement					
		Bar diameter [mm]			
		20	10	8	6
Yield strength	f_y [MPa]	561.5	600.2	560.7	566.2
Ultimate tensile strength	f_t [MPa]	656.7	670.0	623.5	599.7
Ultimate strain	ε [-]	0.078	0.040	0.049	0.015

Tab. 5 *Material properties of prestressing strands*

Prestressing strands			
Cross-section area of strand	A_p	15.7	[mm^2]
Tensile strength	f_p	1840.0	[MPa]
0.1% proof-stress of prestressing steel	f_{p01}	1695.1	[MPa]
Modulus of elasticity	E_p	198.0	[GPa]

3 NLFEM MODEL – DISCRETE REINFORCEMENT

A model with discretely modelled reinforcing and prestressing steel (Figure 6) was created in Atena GiD 15.0.3 and analysed using Atena Studio 5.9.2 software. The model's shape, including the FEM mesh, is shown in Figure 5. For the nonlinear analysis, the creep module was used because the static module exhibited a high degree of the model´s stiffness compared to the experimental results.

The structural scheme of the model is a simply supported beam. The beam's supports are modelled using steel plates with dimensions of 400 x 150 x 30 mm and a high modulus of elasticity to eliminate any plate deformations. The boundary conditions for the supports were as follows:

- Support 1: Line hinge support with no horizontal displacement.
- Support 2: Line hinge support with horizontal displacement allowed.

The calculations of the nonlinear analysis are divided into three intervals:

1. In the first interval, the mass of the beam, including its self-weight, supports, and prestressing, is activated.

2. The second interval simulates the shrinkage and creep of the specimen for a duration of 30 days.

3. In the third interval, the specimen is loaded by deformations in 0.2 mm increments until failure.

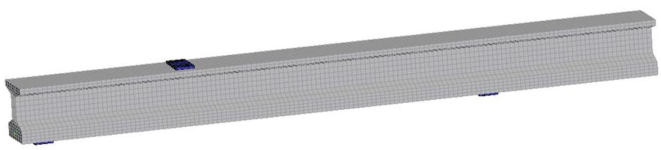

Fig. 5 *3D view of FEM Atena model with mesh and supports*

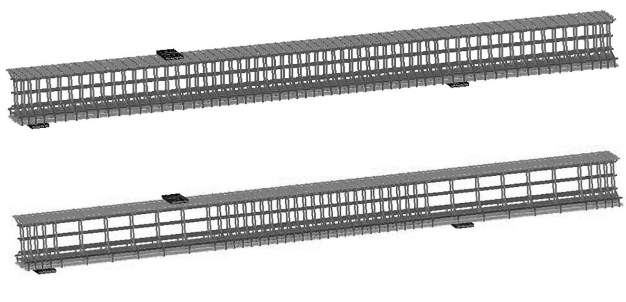

Fig. 6 *Reinforcement of the beams in the Atena model: Specimen N1(top), Specimen N2 (bottom)*

4 NLFEM MODEL – SMEARED REINFORCEMENT

The model with the smeared reinforcing and prestressing steel was created using text commands in Fortran software, which also performed the analysis of the specimens based on Fernando Gonzalez-Vidosa's model (Vidosa 1989). This model is referred to as the ´´UPV model´´ in this paper. Prestressing of the specimen was applied in the model via an axial force acting along the beam's neutral axis. During the calibration of the model with the experimental results, a shear resistance factor of 0.001 was introduced. The model was loaded in 20 kN increments until failure of the specimen. Only half of the section was modelled and loaded; the resulting resistance value was then doubled to obtain the final resistance of the real specimen. The model's shape and its structural scheme are presented in Figure 7.

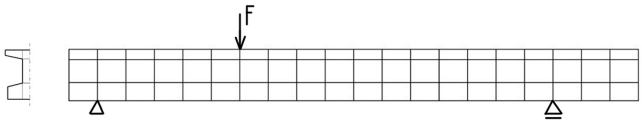

Fig. 7 *Structural scheme and shape of the model: cross-section (left), side view (right)*

5 PARAMETRIC STUDY – EFFECT OF THE AXIAL FORCE

This parametric study investigates the effect of the specimen's prestressing level on its shear resistance obtained using both the ATENA and UPV NLFEM models. The prestressing levels examined in this study ranged from 5% to 100 % of the full prestress of the beam, with the detailed values presented in Table 6.

Fig. 8 *Experimental specimens*

Tab. 6 *Prestressing levels examined*

Level of prestressing	Prestressing stress in the strand	Total prestressing force	Area of concrete cross-section	Axial stresses from prestressing
[%]	[MPa]	[kN]	[m^2]	[MPa]
100	1300	1950.0	0.221	8.82
75	975	1462.5		6.62
50	650	975.0		4.41
25	325	487.5		2.21
5	65	97.5		0.44

The results obtained from the ATENA model are indexed as ´´AT´´, while those from the UPV model are indexed as ´´UPV´´. In addition to the results of the parametric study, the results presented in sections 5.1 to 5.4 also include the results of the experimental testing of the type N1 and N2 beams with the prestressing of 100% and 5% applied. The results of the experimental tests are marked with the EXP symbol in Figures 10 to 20. The experimental specimens of the beams are shown in Figure 8.

The sample labelling scheme, which depends on their shear reinforcement ratio and the level of the prestress, is shown in Figure 9.

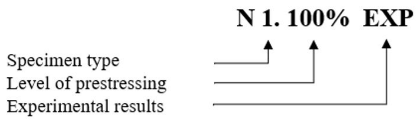

Fig. 9 Sample labelling scheme

5.1 Results – Atena Model – Sample N1

Figures 10 and 11 compare the maximum force applied and the shear resistance obtained experimentally for the beam with a higher shear reinforcement ratio (N1) against the results from the nonlinear Atena model. The experimental shear resistance aligns well with the NLFEM predictions.

At a 100% prestress, the experimental shear resistance is $V_{R,test}$ = 828 kN, while the model predicts V_{AT} = 792 kN, which gives a reliability ratio of $V_{R,test/VAT}$ = 1.045. At a 5% prestress, the experimental value is $V_{R,test}$ = 726 kN, while the model predicts V_{AT} = 693 kN, which results in a ratio of 1.048. The effect of the axial force on the shear resistance observed in the experiments corresponds to an increase from 726 kN to 828 kN, i.e., a 14% increase.

Figure 12 illustrates the relationship between the deformations and force applied. The effect of the axial force is evident through the increased stiffness caused by the delayed formation of the bending cracks. Overall, the experimental results show good agreement with the corresponding NLFEM Atena simulations.

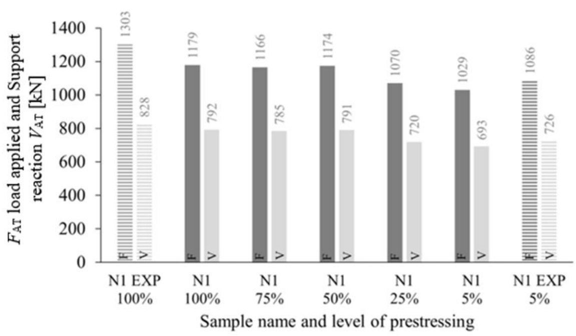

Fig. 10 Maximum applied force F_{AT} and corresponding support reaction V_{AT}

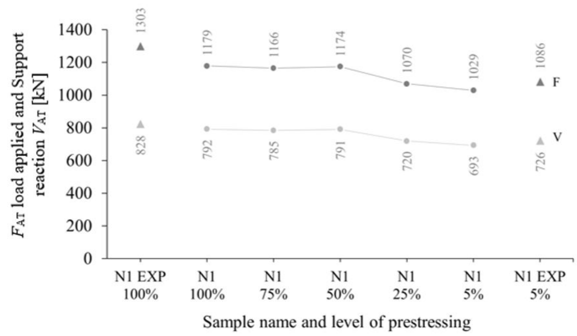

Fig. 11 Relationship of the applied force F_{AT}, the corresponding support reaction (shear resistance) $V_{R.AT}$, and the specimen´s level of prestress

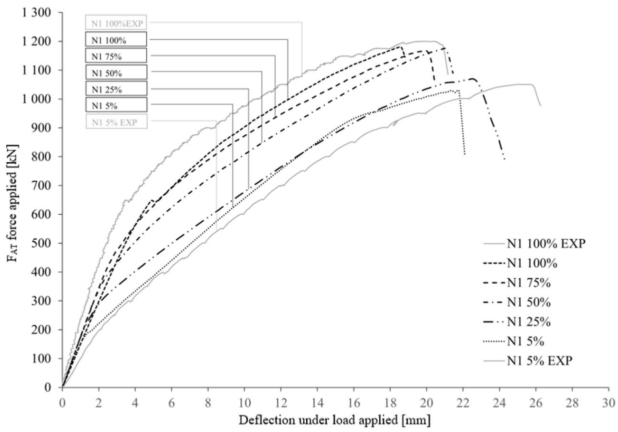

Fig. 12 Force-deflection diagram for specimen N1 ($\rho_{sw,N1}$=0.477) for varying prestress levels

5.2 Results – Atena Model – Sample N1

Figures 13 and 14 compare the maximum force applied and the shear resistance obtained experimentally for a beam with a lower shear reinforcement ratio (N2) against the results from the nonlinear Atena model. The shear resistance obtained experimentally is in good agreement with the NLFEM results. The nonlinear analysis slightly overestimates the experimental resistance.

At a 100% prestress, the experimental shear resistance is $V_{R,test}$ = 567 kN, while the model predicts V_{AT} = 625 kN, giving a reliability ratio of $V_{R,test}/V_{AT}$ = 0.907. At a 5% prestress, the experimental value is $V_{R,test}$ = 441 kN, and the model predicts V_{AT} = 513 kN, resulting in a ratio of 0.048. The effect of the axial force on the shear resistance observed in the experiments corresponds to an increase from 441 kN to 567 kN, i.e., a 29% increase.

Figure 15 illustrates the relationship between the deformations and force applied. The effects of the axial force are evident through the increased stiffness, which is caused by the delayed formation of the bending cracks. Overall, the experimental results show good agreement with the corresponding NLFEM Atena simulations. Due to the low amount of the shear reinforcement, the curve progression, when compared to sample N1, is characterized by several jumps caused by the sudden changes in the stiffness when new cracks form.

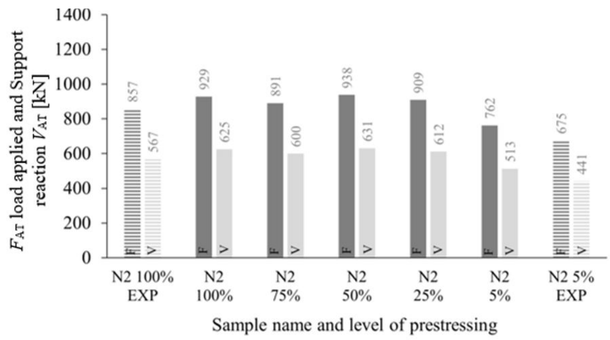

***Fig. 13** Maximum applied force F_{AT} and the corresponding support reaction (shear resistance) $V_{R.AT}$*

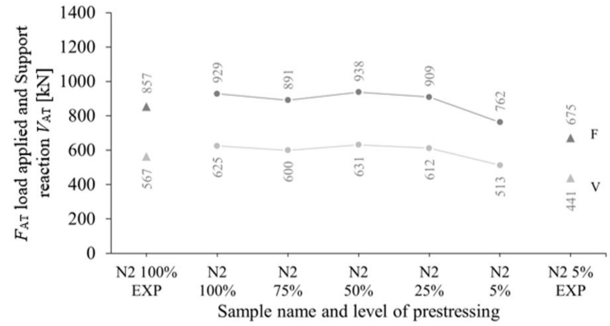

***Fig. 14** Relationship of the force F_{AT} applied, corresponding support reaction (shear resistance) $V_{R.AT}$, and the specimen´s prestress level*

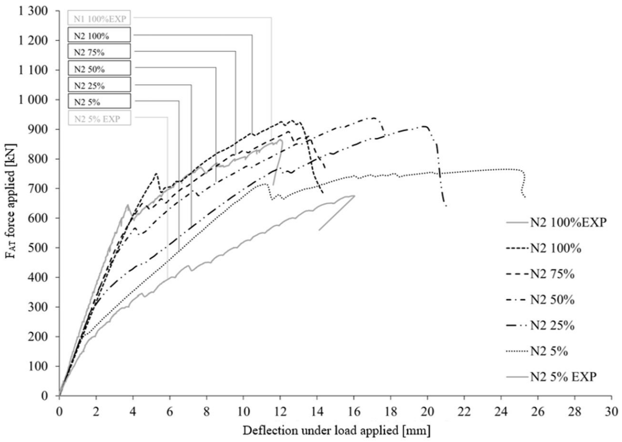

***Fig. 15** Force-deformation diagram for specimen N2 ($\rho_{sw,N1}$=0.105) for varying prestress levels*

5.3 Results – Atena Model – Sample N13

The shear resistance values obtained from the UPV models can be considered safe from a design perspective. The comparison for beam N1 is shown in Figures 16 and 17. At a 100% prestress, the nonlinear model predicts a shear resistance of V_{UPV} = 482 kN, which results in a reliability ratio of $V_{R,test}/V_{UPV}$ = 1.718. For the specimen with the 5% prestress, the model predicts VUPV = 563 kN, with a corresponding reliability ratio of 1.290. Figure 18 illustrates the relationship between the deformations and the force applied. While the nonlinear model UPV accurately reflects the stiffness of the specimens, it predicts failure significantly earlier, i.e., at lower deformation levels compared to the experimental results. The resistance of specimen N1 100%, as analysed by the UPV model, is lower compared to the specimens with a reduced level of prestress, due to the failure of the concrete in compression occurring immediately after the formation of a flexural crack.

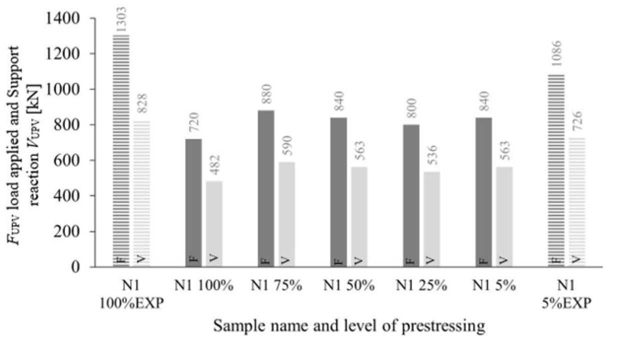

***Fig. 16** Maximum applied force F_{UPV} and corresponding support reaction (shear resistance) $V_{R.UVP}$*

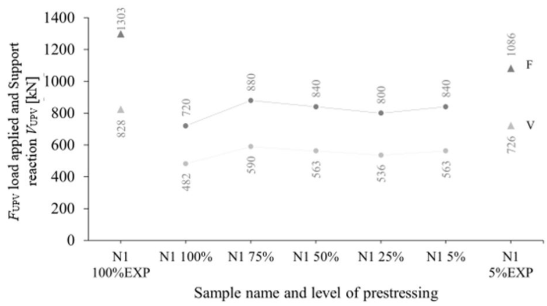

***Fig. 17** Relationship of the force F_{AT} applied, the corresponding support reaction (shear resistance) $V_{R.UPV}$, and the specimen´s prestress level*

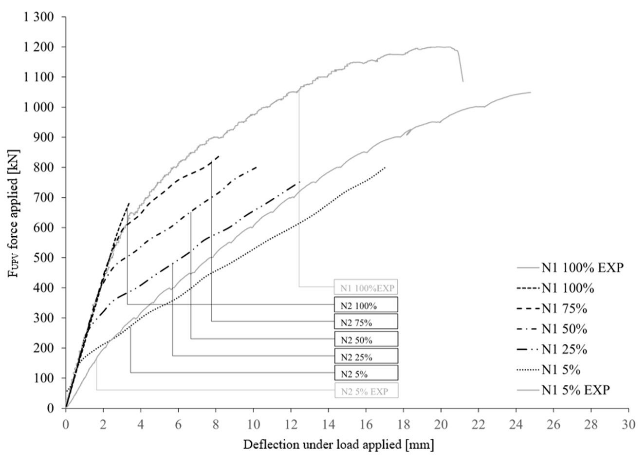

***Fig. 18** Force-deformation diagram for specimen N2 ($\rho_{sw,N1}$=0.105) for varying levels of prestress*

5.4 Results – UPV model – Sample N2

The comparison of the results for the beam with a lower degree of shear reinforcement presented in Figures 19 to 21 is very similar to that of beam N1. At a 100% prestress, the nonlinear model predicts a shear resistance of V_{UPV} = 416 kN, which results in a reliability ratio of $V_{R,test}/V_{UPV}$ = 1.363. For the specimen with the 5% prestress, the model predicts V_{UPV} = 494 kN, with a corresponding reliability ratio of 1.120.

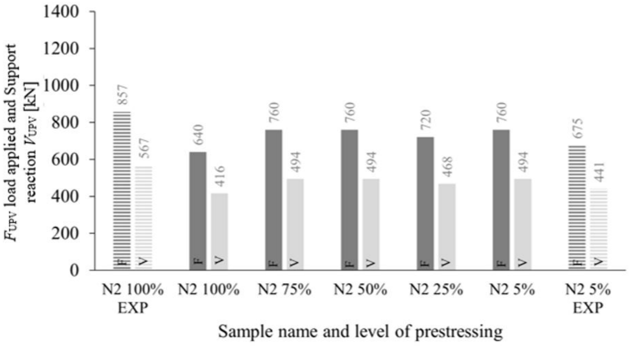

Fig. 19 *Maximum applied force* F_{AT} *and corresponding support reaction (shear resistance)* $V_{R.UPV}$

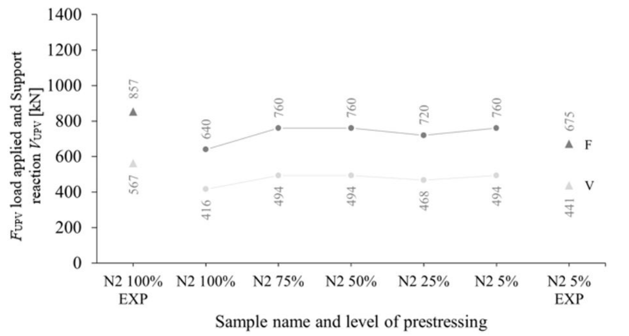

Fig. 20 *Relationship of the force* F_{AT} *applied, corresponding support reaction (shear resistance)* $V_{R.UPV}$ *, and the specimen´s prestress level*

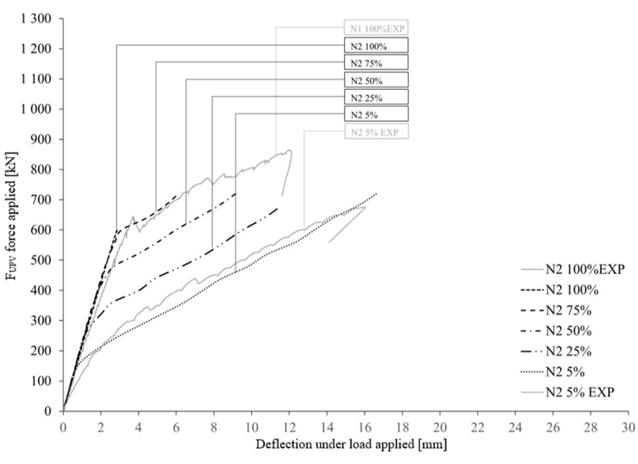

Fig. 21 *Force-deformation diagram for specimen N2 (*$\rho_{sw,N1}$*=0.105) with varying prestresses*

6 CONCLUSIONS

This parametric study on the effect of prestressing on shear resistance, which was conducted using Atena software, demonstrates a clear relationship between the magnitude of the prestress of the cross-section and its shear resistance.

For the specimens with a higher shear reinforcement ratio (N1 samples with $\rho_{sw,N1}$ = 0.477%), at a 5% prestressing level, the element's resistance reached 87% compared to the specimen with a 100% prestressing level. The most significant drop in shear resistance occurred between the 50% and 25% prestressing levels.

For the specimens with a low shear reinforcement ratio (N2 samples with $\rho_{sw,N2}$ = 0.104%), at a 5% prestressing level, the element exhibited 82% resistance compared to the specimen with a 100% prestressing level. Here, the largest decrease in shear resistance was observed between the 25% and 5% prestressing levels.

The parametric study on the effect of prestressing on shear resistance, which was performed using the UPV model, indicated that the UPV model does not account for the effect of the axial force on its shear resistance. The effect of prestressing in this model was manifested by an increased flexural stiffness of the elements, thereby leading to a later onset and development of cracks. Based on the results of the parametric study conducted with the Atena model, it can be concluded that for specimens with a higher degree of shear reinforcement, a complete loss of prestress will lead to a 13% decrease in shear resistance. For specimens with a low degree of shear reinforcement, a complete loss of prestress will result in an 18% decrease in shear resistance.

Acknowledgments

This work was supported by the Scientific Grant Agency VEGA under Contract No. VEGA 1/0358/23.

REFERENCES

BELLETTI, Beatrice et al. (2020). *Experimental tests on shear capacity of naturally corroded prestressed beams.* Structural concrete, pp. 1-17. Available at: https://doi.org/10.1002/suco.202000205

MORAVČÍK, Martin; Petra BUJŇÁKOVÁ, František BAHLEDA (2020). *Failure and damage of a first-generation precast prestressed bridge in Slovakia.* Structural concrete. 2020; 21:2353-2362; https://doi.org/10.1002/suco.201900526

ČERVENKA, Vladimír; Jan ČERVENKA. ATENA *Program Documentation Part 2-2 – User´s Manual for ATENA 3D. (2017)***.** Available at: https://www.cervenka.cz/products/atena/documentation

HERBRAND, Martin; Josef HEGGER (2013). *Experimental studies on the shear capacity of Prestressed Concrete Continuous Beams.* IABSE Conference Rotterdam 2013, Report Vol. 99, pp. 84-85 (short paper). ISBN 978-3-85748-123-9

HERBRAND, Martin (2017). *Shear strength models for reinforced and prestressed concrete members.* Dissertation thesis. Aachen. RWTH Aachen University. DOI:10.18154/RWTH-2017-06170

HUBER, Patrick et al. (2018). *Influence of loading conditions on the shear capacity of post-tensioned beams with low shear reinforcement ratios.* Engineering Structures 170, pp. 91-102. Available at: https://doi.org/10.1016/j.engstruct.2018.05.079

HILLEBRAND, Matthias; Viviane Adam; Martin Classen; Josef Hegger. *Fatigue of Shear Reinforcement in Prestressed Concrete I- and T-Beams under Cyclic Loading.* Conference: fib Symposium 2019: Concrete - Innovations in Materials, Design and Structures. Cracow, Poland;

RUPF, Michael et al. (2013). P*ost-tensioned girders with low amounts of shear reinforcement: Shear strength and influence of flanges.* Engineering Structures 56, pp. 357-371. Available at: http://dx.doi.org/10.1016/j.engstruct.2013.05.024

GONZÁLEZ-VIDOSA, Fernando (1989) *Three-dimensional finite element analysis of structural concrete understatic loading.* Dissertation thesis. London. University of London, Imperial College of Science of Technology and Medicine.